**New Journal of Physics**
The open access journal at the forefront of physics

Deutsche Physikalische Gesellschaft DPG
IOP Institute of Physics

Published in partnership with: Deutsche Physikalische Gesellschaft and the Institute of Physics

CrossMark

OPEN ACCESS

RECEIVED
18 January 2022

REVISED
20 March 2022

ACCEPTED FOR PUBLICATION
8 April 2022

PUBLISHED
5 May 2022



PAPER

# Segregation dynamics driven by network leaders

**Wenxuan Wang[1], Yuhao Feng[1], Siru Chen[1], Wenzhe Xu[1], Xinjian Zhuo[1], Hui-Jia Li[1,*] and Matjaž Perc[2,3,4,5,*]**

[1] School of Science, Beijing University of Posts and Telecommunications, Beijing 100876, People's Republic of China
[2] Faculty of Natural Sciences and Mathematics, University of Maribor, Koroška cesta 160, 2000 Maribor, Slovenia
[3] Department of Medical Research, China Medical University Hospital, China Medical University, Taichung 404332, Taiwan
[4] Alma Mater Europaea, Slovenska ulica 17, 2000 Maribor, Slovenia
[5] Complexity Science Hub Vienna, Josefstädterstraße 39, 1080 Vienna, Austria
[*] Authors to whom any correspondence should be addressed.

**E-mail:** **Hjli@bupt.edu.cn** and **matjaz.perc@gmail.com**

**Keywords:** complex networks, network segregation, multi-agent leader–follower consensus system, key leaders identification

Supplementary material for this article is available online

## Abstract

Network segregation—a critical problem in real-life networks—can reveal the emergence of conflicts or signal an impending collapse of the whole system. However, the strong heterogeneity of such networks and the various definitions for key nodes continue to pose challenges that limit our ability to foresee segregation and to determine the main drivers behind it. In this paper, we show that a multi-agent leader–follower consensus system can be utilized to define a new index, named leadership, to identify key leaders in real-life networks. And then, this paper explores the emergence of network segregation that is driven by these leaders based on the removal or the rewiring of the relations between different nodes in agreement with their contribution distance. We finally show that the observed leaders-driven segregation dynamics reveals the dynamics of heterogeneous attributes that critically influence network structure and its segregation. Thus, this paper provides a theoretical method to study complex social interactions and their roles in network segregation, which ultimately leads to a closed-form explanation for the emergence of imbalanced network structure from an evolutionary perspective.

## 1. Introduction

Cooperation and conflict are essential characteristics of contemporary social relations, significantly influencing international relations and interpersonal relationships. The typical social relations mainly reflect that people with similar characteristics are more closely connected than people without similar characteristics. These network characteristics have been shown in a variety of situations [1–3], such as high school friendship network segregation by race and gender factors [4], as well as environmental policy network segregation by values and faith [5]. Network segregation is defined as 'the degree to which two or more groups live separately from one other' [6]. In many real systems, cooperation and conflict are the core features that cause network segregation in many policy issues, such as public administration, climate policy, and economic regulation and control [7, 8]. Thus, exploring the dynamics of network segregation becomes an important and attractive topic now [9, 10].

Generally speaking, real social networks are highly heterogeneous and sophisticate [11]. It is unrealistic to assume that individual contribution is uniformly distributed in many practical problems. Especially residential segregation [12, 13], which is driven by inconsistent variables such as race or social relations [14, 15]. Heterogeneous individuals have different contribution values. Motivated by the famous Karate network [16], this paper originally introduces the role of 'key leaders' to drive network segregation. The key leader is an organization member or a decision-maker who can promote consensus among members.

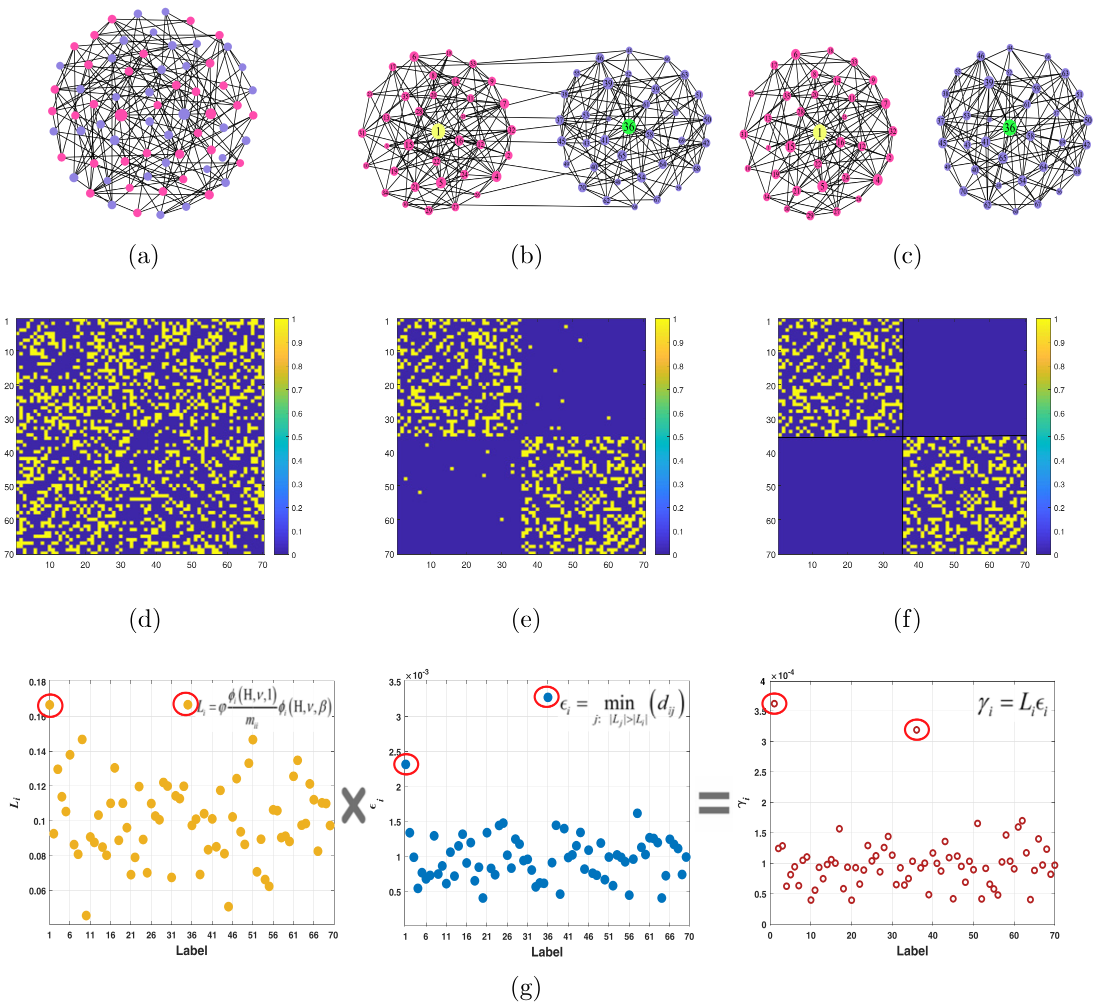

**Figure 1.** The segregation dynamics in networks driven by key leaders. (a)–(c) The network representation of (a) a complete mixing network with a size of $N = 70$, (b) a mixing network after removing and rewiring, and (c) a complete segregated network. (d)–(f) Are corresponding matrix representations of (a)–(c), respectively. The black lines represent boundaries of different groups. (g) The $L_i$, $\epsilon_i$ and $\gamma_i$, of each node $i$ of the network during an iteration. Here, $L_i = \varphi\frac{\phi_i(\mathbf{H},v,1)}{m_{ii}}\phi_i(\mathbf{H},v,\beta)$, Reaction Distance $\epsilon_i = \min_{j:|L_j|>|L_i|}(d_{ij})$, and *leadership* $\gamma_i = L_i\epsilon_i$ for *i*.

Therefore, their decision is responded to by other followers. However, previous studies have ignored the heterogeneous characteristic in real networks.

In addition, the existing researches consider network segregation through identifying the local structures such as community structure or motif [17–19]. The emergence of community or motif is the result of network segregation, which is caused by complex social relations, public policies, or economic inequality [20]. They only focus on how to identify key leaders [21] and how different characteristics of participants interact with each other [22, 23], respectively. However, community detection or motif finding only focus on a local structure, not revealing the hidden dynamical behaviours of the collective response system.

To explore how key leaders drive network segregation, we utilize a leader–follower consensus system [24] to simulate social patterns. The segregation dynamics are shown in figure 1. Firstly, we show that the leader–follower consensus system has a higher contribution value increment than distributed linear consensus system. The evolution of individual behaviour is explored in social networks. Secondly, we propose a new index to characterize key leaders, denoted as *leadership*, which can be extended to many famous centrality indexes, such as degree centrality (DC), closeness centrality (CC), Katz centrality, etc. Thirdly, we design a dynamic process to explain the emergence of network segregation and further reveal the responsiveness of collective dynamics after the key leaders are identified. The state at nodes and segregated processes is predicted by dynamical process. Finally, we perform multi-type numerical experiments on real and artificial networks to validate the effectiveness of our method.

## 2. Methods

### 2.1. Distributed linear consensus system

In this paper, to reveal the hidden dynamical behaviours of heterogeneous systems, we apply the distributed linear consensus system [25] in the social network, and each node of the network represents an agent, denoted by $i$. The linear consensus system represents a rich phenomenon that the contribution values of agents rely on the time scale. Especially, the system describes the dynamic process of information exchange between each agent and its neighbours. Let us consider the case in which a group of $N$ agents with a particular distributed consensus protocol and the scalar contribution value $x_i(t)$ measures the state of $i$ at time $t$. The system's dynamics is defined by the state vector $\mathbf{X}(t) = (x_i(t))_{N\times 1}$ for $i = 1, \ldots, N$ and the adjacency matrix $\mathbf{A} = (a_{ij})_{N\times N}$ for $i, j = 1, \ldots, N$ where the value of $a_{ij} = 1$ if agent $i$ is connected to $j$ and zero otherwise. Given a network, the system evolves according to the following model:

$$\frac{\mathrm{d}x_i}{\mathrm{d}t} = \beta_i + \frac{\omega_0}{k_i}\sum_{j=1}^{N} a_{ij}\left(x_j(t) - x_i(t)\right) = \beta_i + \sum_{j=1}^{N} w_{ij}x_j(t), \tag{1}$$

where the natural response frequency is $\omega_0$, the degree of agent $i$ is $k_i = \sum_{j=1}^{N} a_{ij}$. And then $w_{ij} = \omega_0\left(a_{ij}/k_i - \delta_{ij}\right)$. For all $i, j = 1, \ldots, N$, using the Kronecker symbol $\delta_{ij}$.

The equation (1) can be rewritten in matrix on the frequency domain as

$$\mathbf{X}(\omega) = (i\omega\mathbf{I} - \mathbf{W})^{-1}\boldsymbol{\beta}, \tag{2}$$

where $\mathbf{I}$ is an identity matrix for the size of $N \times N$, the $N \times N$ state matrix between the agent is denoted by $\mathbf{W}$, and $\beta$ is a weight vector, representing the ability in certain cases. Simplified as: $\boldsymbol{\delta} = \omega i$. We define the index $\Phi(\mathbf{W}, \delta, \beta) = (\delta\mathbf{I} - \mathbf{W})^{-1}\beta$ as the weighted Katz centrality with parameter $\frac{1}{\delta}$ and weight vector $\beta$. We find that equation (2) equivalent to solve $\frac{\partial u_i}{\partial x_i} = 0$ for all agents $i$ on the frequency domain, where

$$u_i = \beta_i x_i - \frac{1}{2}(\delta - \omega_0)x_i^2 + \sum_{j=1}^{N} w_{ij}x_i x_j. \tag{3}$$

### 2.2. Leader–follower consensus system

To model the system's response driven by key leaders, we consider a leader–follower consensus system, which has two stages. In the first stage, the key leaders move first. In the second stage, by observing the contribution of key leaders, other agents consider following them. The key leaders are generally regarded as thought leaders or decision-makers in this leader–follower consensus system. The agents are divided into two groups, i.e., the leader node set $\mathbb{L}$ and the follower node set $\mathbb{F}$. We consider the leader–follower consensus system with $|\mathbb{L}|$ leaders and $|\mathbb{F}|$ followers. These agents do not satisfy the dynamics of equation (1), but instead follow contribution values $x_i = x_i^{\mathrm{L}}$ $(\forall i \in \mathbb{L})$ and $x_i = x_i^{\mathrm{F}}$ $(\forall i \in \mathbb{F})$.

$$\begin{cases} \dfrac{\mathrm{d}x_i^{\mathrm{L}}}{\mathrm{d}t} = \beta_i^{\mathrm{L}} + \left(\displaystyle\sum_{j\in\mathbb{L}} w_{ij}x_j^{\mathrm{L}} + \sum_{j\in\mathbb{F}} w_{ij}x_j^{\mathrm{F}}\right) & \forall i \in \mathbb{L} \\ \dfrac{\mathrm{d}x_i^{\mathrm{F}}}{\mathrm{d}t} = \beta_i^{\mathrm{F}} + \left(\displaystyle\sum_{j\in\mathbb{L}} w_{ij}x_j^{\mathrm{L}} + \sum_{j\in\mathbb{F}} w_{ij}x_i^{\mathrm{F}}\right) & \forall i \in \mathbb{F}. \end{cases} \tag{4}$$

We denote $\mathbf{X}_{\mathrm{L}} = (x_i^{\mathrm{L}})_{|\mathbb{L}|\times 1}$ $(\forall i \in \mathbb{L})$ and $\mathbf{X}_{\mathrm{F}} = (x_i^{\mathrm{F}})_{|\mathbb{F}|\times 1}$ $(\forall i \in \mathbb{F})$ as the contribution values of leader and follower node vector, respectively. The contribution of followers $\mathbf{X}_{\mathrm{F}}$ in matrix on the frequency domain as

$$\mathbf{X}_{\mathrm{F}}(\omega) = (i\omega\mathbf{I} - \mathbf{W}_{\mathrm{FF}})^{-1}(\boldsymbol{\beta}_{\mathrm{F}} + \mathbf{W}_{\mathrm{FL}}\mathbf{X}_{\mathrm{L}}), \tag{5}$$

where $\mathbf{I}$ is an identity matrix for the size of $N \times N$. $|\mathbb{F}|$ and $|\mathbb{L}|$ are the number of leaders and followers. $\mathbf{W}_{\mathrm{FF}}$ is a $|\mathbb{F}| \times |\mathbb{F}|$ state matrix between the followers. $\mathbf{W}_{\mathrm{FL}}$ is a $|\mathbb{F}| \times |\mathbb{L}|$ state matrix between the leaders and the followers. $\beta_{\mathrm{F}}$ is a weight vector of followers, representing the ability in certain cases. $X_{\mathrm{L}}$ can be mapped to $X_{\mathrm{F}}$ by a linear transformation.

Since the contribution's difference between distributed linear consensus system and leader–follower consensus system is difficult to be calculated by a single matrix form directly, it can be equivalently converted into $\frac{\partial u_i}{\partial x_i} = 0$, where

$$u_i = \begin{cases} \beta_i^{\mathrm{L}} x_i^{\mathrm{L}} - \frac{1}{2}(\delta - \omega_0)(x_i^{\mathrm{L}})^2 + x_i^{\mathrm{L}} \left( \sum_{j \in \mathbb{L}} w_{ij} x_j^{\mathrm{L}} + \sum_{j \in \mathbb{F}} w_{ij} x_j^{\mathrm{F}} \right) & \forall i \in \mathbb{L} \\ \beta_i^{\mathrm{F}} x_i^{\mathrm{F}} - \frac{1}{2}(\delta - \omega_0)(x_i^{\mathrm{F}})^2 + x_i^{\mathrm{F}} \left( \sum_{j \in \mathbb{L}} w_{ij} x_j^{\mathrm{L}} + \sum_{j \in \mathbb{F}} w_{ij} x_j^{\mathrm{F}} \right) & \forall i \in \mathbb{F}. \end{cases} \tag{6}$$

In order to obtain the increment of the contribution values from distributed linear consensus system to leader–follower consensus system, we firstly calculate the agent's contribution values based on equation (6). To simplify the representation of the vector $\mathbf{X}$, the contribution values of nodes in $\mathbb{L}$ and $\mathbb{F}$ are denoted as vector $\mathbf{X}_{\mathrm{L}}$ and $\mathbf{X}_{\mathrm{F}}$, and $\mathbf{X}$ can be rewritten as a block vector: $\mathbf{X} = (\mathbf{X}_{\mathrm{L}}, \mathbf{X}_{\mathrm{F}})^{\mathrm{T}}$. Let $\mathbf{H} = \mathbf{W} - \mathbf{W}^{\mathrm{D}}$ and $v = \delta + \omega_0$. And the matrix $\mathbf{H}$ can be rewritten as a block matrix:

$$\mathbf{H} = \begin{pmatrix} \mathbf{H}_{\mathrm{LL}} & \mathbf{H}_{\mathrm{LF}} \\ \mathbf{H}_{\mathrm{FL}} & \mathbf{H}_{\mathrm{FF}} \end{pmatrix}. \tag{7}$$

By applying the backward induction method, when $v$ is big enough, we obtain the agent's contribution values of the leader–follower consensus system by

$$\begin{pmatrix} \mathbf{X}_{\mathrm{L}} \\ \mathbf{X}_{\mathrm{F}} \end{pmatrix} = \mathbf{S} \begin{pmatrix} \beta_{\mathrm{L}} \\ \beta_{\mathrm{F}} \end{pmatrix}, \tag{8}$$

with

$$\mathbf{S} = \begin{pmatrix} [v\mathbf{I} - (\mathbf{T} + \mathbf{T}^{\mathrm{D}})]^{-1} & [v\mathbf{I} - (\mathbf{T} + \mathbf{T}^{\mathrm{D}})]^{-1}\mathbf{H}_{\mathrm{LF}}\mathbf{U} \\ \mathbf{U}\mathbf{H}_{\mathrm{FL}}[v\mathbf{I} - (\mathbf{T} + \mathbf{T}^{\mathrm{D}})]^{-1} & \mathbf{U} + \mathbf{U}\mathbf{H}_{\mathrm{FL}}[v\mathbf{I} - (\mathbf{T} + \mathbf{T}^{\mathrm{D}})]^{-1}\mathbf{H}_{\mathrm{LF}}\mathbf{U} \end{pmatrix}, \tag{9}$$

where $\mathbf{T} = \mathbf{H}_{\mathrm{LL}} + \mathbf{H}_{\mathrm{LF}}\mathbf{U}\mathbf{H}_{\mathrm{FL}}$, $\mathbf{T}^{\mathrm{D}}$ is the diagonal matrix of $\mathbf{T}$ whose main diagonal components $\mathbf{T}_{ii}^{\mathrm{D}} = t_{ii},\ i = 1, \dots, n$ and off diagonal components $\mathbf{T}_{ij}^{\mathrm{D}} = 0,\ \forall\ i \neq j$, $\mathbf{U} = [v\mathbf{I} - \mathbf{H}_{\mathrm{FF}}]^{-1}$, and $\beta = (\boldsymbol{\beta}_{\mathrm{L}}, \boldsymbol{\beta}_{\mathrm{F}})^{\mathrm{T}}$ is a weight vector of leaders and followers, respectively. In addition, if $\mathbf{H}$ is matrix symmetric, $\mathbf{S}$ is symmetric as well. The derivation is presented in supplementary materials (https://stacks.iop.org/NJP/24/053007/mmedia).

Interestingly, one can find that these contribution values can be comprehend in two aspects. Firstly, the contribution values increase linearly with each component of $\beta$, where $\mathbf{S}$ indicates the sensitivities. This implies that each agent's contribution can be influenced positively and directly by other agents' increased intrinsic value. Moreover, matrix $\mathbf{S}$ summarizes the influence extent in a nutshell. Secondly, the sub-sequential responses of followers in the set $\mathbb{F}$ are anticipated.

### 2.3. The index of leadership

The solution to the problem is $\mathbf{X}^N = [v\mathbf{I} - \mathbf{H}]^{-1}\beta$ for a directed linear consensus system. By applying the block matrix inversion formula, the matrix of sensitivities of intrinsic value $\mathbf{M}$ can be rewritten as below:

$$\mathbf{M} = [v\mathbf{I} - \mathbf{H}]^{-1} = \begin{pmatrix} [v\mathbf{I} - (\mathbf{T} + \mathbf{0})]^{-1} & [v\mathbf{I} - (\mathbf{T} + \mathbf{0})]^{-1}\mathbf{H}_{\mathrm{LF}}\mathbf{U} \\ \mathbf{U}\mathbf{H}_{\mathrm{FL}}[v\mathbf{I} - (\mathbf{T}+\mathbf{0})]^{-1} & \mathbf{U} + \mathbf{U}\mathbf{H}_{\mathrm{FL}}[v\mathbf{I} - (\mathbf{T} + \mathbf{0})]^{-1}\mathbf{H}_{\mathrm{LF}}\mathbf{U} \end{pmatrix}. \tag{10}$$

It is confirmable that $\mathbf{S} \succeq \mathbf{M}$. To obtain more quantitative conclusions about the difference between distributed linear consensus and leader–follower consensus system, supposing $v$ is big enough, the increment of contribution values between distributed linear consensus system and leader–follower consensus system. We have

$$\begin{pmatrix} \mathbf{X}_{\mathrm{L}} \\ \mathbf{X}_{\mathrm{F}} \end{pmatrix} - \begin{pmatrix} \mathbf{X}_{\mathrm{L}}^N \\ \mathbf{X}_{\mathrm{F}}^N \end{pmatrix} = \frac{1}{v^2} \begin{pmatrix} (\mathbf{H}_{\mathrm{LF}}\mathbf{H}_{\mathrm{FL}})^{\mathrm{D}} & 0 \\ 0 & 0 \end{pmatrix} \begin{pmatrix} \beta_{\mathrm{L}} \\ \beta_{\mathrm{F}} \end{pmatrix} + O\left(\frac{1}{v^3}\right), \tag{11}$$

where $(\mathbf{X}_{\mathrm{L}}, \mathbf{X}_{\mathrm{F}})^{\mathrm{T}}$ is the contribution vector of leader–follower consensus system, and $(\mathbf{X}_{\mathrm{L}}^N, \mathbf{X}_{\mathrm{F}}^N)^{\mathrm{T}}$ is the contribution vector of distributed linear consensus system. And the parameter $v = \delta + \omega_0$.

The proof of equation (11) is presented in supplementary materials. Equation (11) implies that the leader–follower consensus system makes use of the positive feedback productively. Especially, the agent's contribution is higher (lower if $\beta_{\mathrm{L}}$ is negative) than the distributed linear consensus system, without respect to the potential network structure. Equation (11) expresses the incremental benefit of the leader–follower consensus system concisely. In equation (11), the first significant term shows a common linear term between these two contribution vectors. The square term $\left((\mathbf{H}_{\mathrm{LF}}\mathbf{H}_{\mathrm{FL}})^{\mathrm{D}}, 0\right)^{\mathrm{T}}$ is only up to $\beta_{\mathrm{L}}$, but is not influenced by $\beta_{\mathrm{F}}$.

To recognize the key leaders, we consider a leader–follower consensus system and use the criterion of aggregate contribution. Intuitively, we measure the influence extent for the whole network when the leader becomes a regular follower. Specifically, if we change a leader to a follower and it has little difference for other nodes, we ignore this node's influence, and it is more suitable as a follower. Otherwise, this node is critical and is more suitable as a leader. In the first stage of the leader–follower consensus system, a specific leader $i$ moves first, and the other agents (followers) move in the second stage. For a leader $i$, we get the contribution:

$$x_i^{\mathrm{L}} = \frac{\beta_i + \langle v_i, (v\mathbf{I} - \mathbf{H}_{-i})^{-1}\beta_{-i}\rangle}{1 - 2\langle v_i, (v\mathbf{I} - \mathbf{H}_{-i})^{-1}\beta_{-i}\rangle} = \frac{\phi_i(\mathbf{H}, v, \beta)}{2 - m_{ii}}, \tag{12}$$

where $m_{ij} = ((v\mathbf{I} - \mathbf{H})^{-1})_{ij}$, $\phi_i(\mathbf{H}, v, \beta) = \sum_{j=1}^{n} m_{ij}\beta_j$, and $\mathbf{H}$ can be rewritten as below:

$$\mathbf{H} = \begin{pmatrix} 0 & v_i' \\ v_i & \mathbf{H}_{-i} \end{pmatrix}. \tag{13}$$

Moreover, for a agent $i$, the contribution in distributed linear consensus system is given by:

$$x_i^{N} = \frac{\beta_i + \langle v_i, (v\mathbf{I} - \mathbf{H}_{-i})^{-1}\beta_{-i}\rangle}{1 - \langle v_i, (v\mathbf{I} - \mathbf{H}_{-i})^{-1}\beta_{-i}\rangle} = \phi_i(\mathbf{H}, v, \beta). \tag{14}$$

To determine the key leader, we compare the difference to each node between distributed linear consensus system and the leader–follower consensus system. Thus, if a node $i$ is selected as a leader, the difference of aggregate contribution values between distributed linear consensus system and leader–follower consensus system is

$$\begin{aligned} L_i &= \left\{ x_i^{\mathrm{L}} + \sum_{j \neq i} x_j^*(x_i^{\mathrm{L}}) \right\} - \left\{ x_i^{N} + \sum_{j \neq i} x_j^*(x_i^{N}) \right\} \\ &= \left( 1 + \sum_{j \neq i} \frac{m_{ij}}{m_{ii}} \right) (x_i^{\mathrm{L}} - x_i^{N}) \\ &= \varphi \frac{\phi_i(\mathbf{H}, v, 1)}{m_{ii}} \phi_i(\mathbf{H}, v, \beta), \end{aligned} \tag{15}$$

where $\varphi = \frac{(m_{ii}-1)}{(2-m_{ii})}$, $x_j^*(\cdot)$ is an affine function of $x_i$.

We find that $L_i$ is inversely proportional to $m_{ii}$, which means the leaders' influence should be extended to other agents instead of returning towards itself. In addition, the variable $\phi_i(\mathbf{H}, v, \beta)$ is called weighted Katz–Bonacich centrality [26] of parameter $v$ and weight vector $\beta$. $L_i$ is proportional to $\phi_i(\mathbf{H}, v, 1)$, which means the influence of key leaders spread easily. Furthermore, it is proportional to $\phi_i(\mathbf{H}, v, \beta)$, which means the leaders should maintain well contact with other agents in their groups. In short, index $L_i$ is a general measure with rich information, which matches many famous centrality indexes, such as DC, betweenness centrality (BC), CC, Katz centrality, etc.

Intuitively, the key leaders should be the innermost nodes in the network, while the other nodes should be distributed around the key leaders [27, 28]. The $\beta$ must be provided in equation (15), which is critical for selecting the key leaders. Here, $\beta_i = (\pm)k_i$ is set, where $k_i$ is the degree of node $i$. Then a bigger $\phi_i(\mathbf{H}, v, \beta)$ indicates that the leader should be well tied to large degree nodes (from within its group) and have the shortest path with the large degree nodes (from within its group). $\beta$ can segregate different levels. The ability to specify different levels can indicate multiple groups and a hierarchical structure.

It is worth notice that the famous density peak theory [29], the locations of leaders should be *disassortative*, which means the leader should have a large distance to other leaders (i.e., the node with a higher index value $L_i$). In contrast, the leaders should have a relatively short distance with their neighbours (i.e., the node with a lower index value $L_i$). Based on this motivation, the notion of *reaction distance* (RD) $\epsilon$ is proposed to identify key leaders. Specifically, the RD of node $i$, $\epsilon_i$, is defined as the minimal distance of

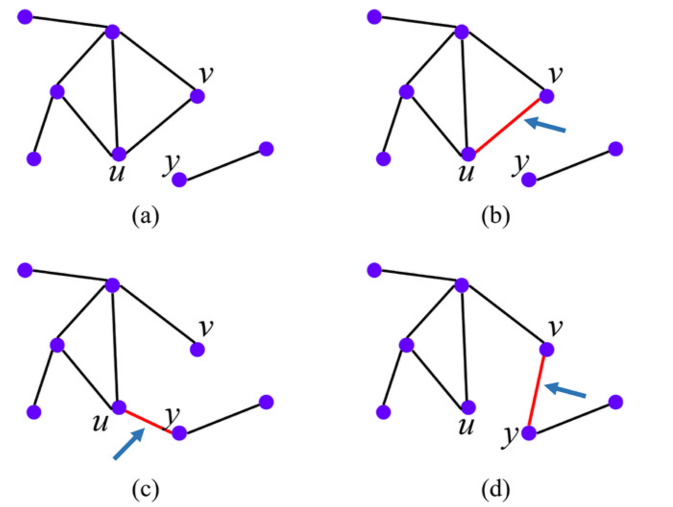


**Figure 2.** A schematic diagram of segregation dynamics driven by key leaders. (a) Is shown that an initial network. (b)–(d) We select one edge *uv* and make a choice to keep (as shown is (b)) or delete the connection (as shown is (c) and (d)) ground on their attribute distance and $p_1$ firstly. Concretely, when the edge *uv* is removed, one node *y* is randomly selected. Lastly, adding either *uy* (as shown is (c)) or *vy* (as shown is (d)) with probability $p_2$ and $p_3$, respectively.

shortest paths from node $i$ to other nodes that have a higher leading index $L_i$,

$$\epsilon_i = \min_{j:|L_j|>|L_i|}(d_{ij}). \tag{16}$$

Here, $d_{ij}$ is the shortest path between node $i$ and node $j$. If the node $i$ has a higher RD, the close neighbours of node $i$ will have a relatively lower absolute value of leading index $L_i$ compared with $i$. If we find a node with higher RD than node $i$, a farther network distance must be searched, implying that it is more likely to be a leader.

For a agent $i$, the *leadership* is defined as

$$\gamma_i = L_i\epsilon_i, \tag{17}$$

where $L_i$ is represented as local connectivity and $\epsilon_i$ is *RD*.

## 3. Segregation dynamics driven by leaders

Based on their evolved attributes, we establish a network segregation model (named as *leader–follower consensus method*, which is abbreviated with **LFC**) by leaders' influences. The network can be segregated into two or more groups. Define the contribution distance between $u$ and $v$ by the function $d(x_u, x_v)$ as *attribute distance* [30], which indicates whether two agents are in the same state. When the agents are fixed in attribute space, the big and small attributes are referred to as the long edges and short edges, respectively. It is consistent between attribute distance and social relations: relations between agents with closely connected are short, while long relations between agents with large social distances.

For a network $\mathcal{G}$ with the node set $\mathbb{V} = 1, 2, \ldots, N$ and the edge set $\mathbb{E} \subseteq \mathbb{V} \times \mathbb{V}$. The evolution dynamics initiate at $t = 0$, and the network $\mathcal{G} = \mathcal{G}_0$. For every time step $t$, an edge $uv \in \mathbb{E}$ is randomly selected to model the process. And then, the attribute distance $d(x_u, x_v)$ is calculated with $u$ and $v$. Depending on the distance, they can decide whether to remove or rewire their connection. Specifically, the dynamical process of conversion from $\mathcal{G}_{t-1}$ to $\mathcal{G}_t$ at the time step $t$ is detailed below. Firstly, we find key leaders with maximal value of leadership $\gamma_i$ (equation (17)). For each node $i$, the contribution value $x_i^{\mathrm{L}}$ as a leader and the contribution value $x_i^N$ as a follower should be calculated by the equations (12) and (14), respectively. Secondly, the distance of two nodes are defined by the difference of their attribute distance, i.e., $d(x_u, x_v) = |x_u - x_v|$, the probability deleting the edge between $u$ and $v$ is $d(x_u, x_v) \cdot p_1$, where $p_1$ is a tuned parameter. When the edge $uv$ is removed, it is then rewired according to the following rules: (1) choosing a node $y \in \mathbb{V}$ uniformly at random; (2) adding either edge $uy$ with a probability $p_2 = \frac{d(x_v,x_y)}{d(x_u,x_y)} \cdot q$ and adding either edge $vy$ with a probability $p_3 = 1 - \frac{d(x_v,x_y)}{d(x_u,x_y)} \cdot q$, where $q$ is a tuned parameter. Figure 2 shows a schematic diagram. We always keep the total number of edges in the network constant during the process. This assumption allows the degree distribution to change. We just believe that the density of the network stays unchanged in the whole dynamical process.

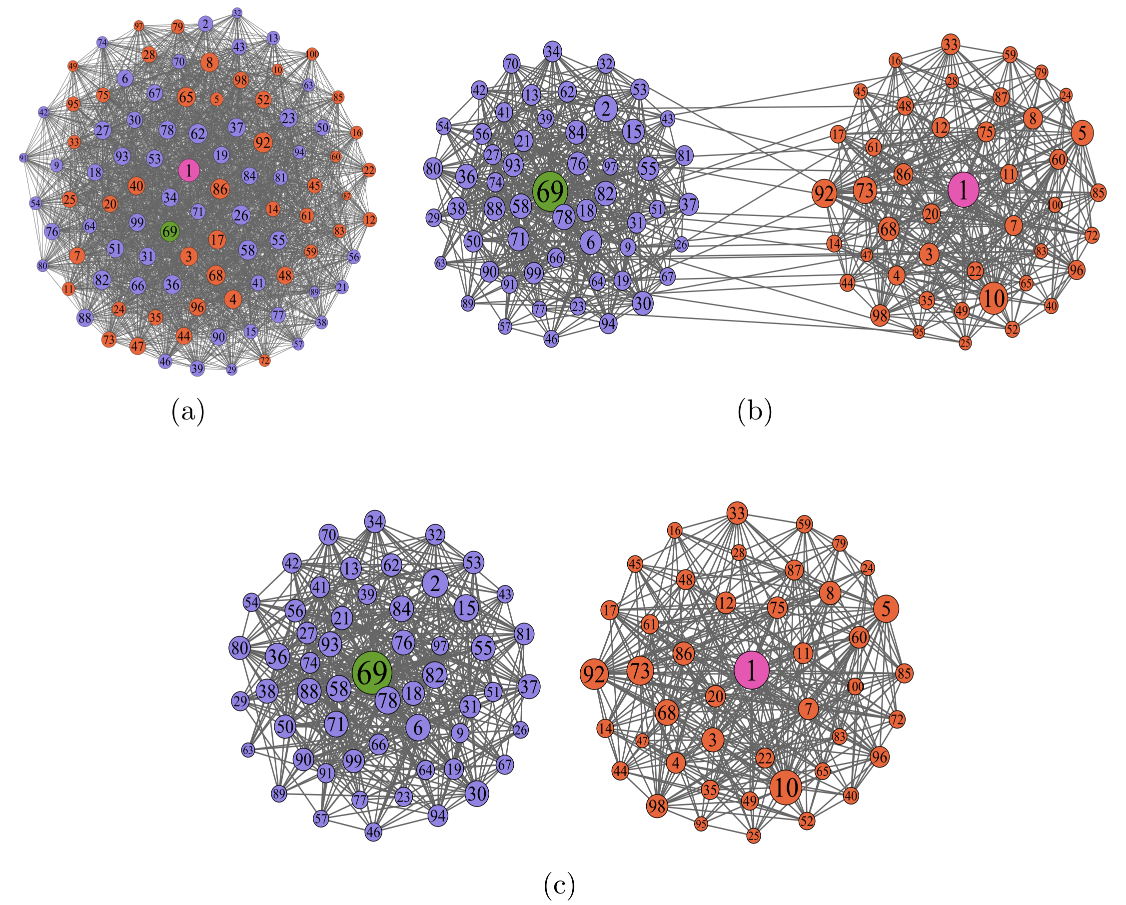


**Figure 3.** The segregation process driven by key leaders in an ER random network. (a) The initial ER random network with 100 nodes and 300 edges. (b) After 200 time steps, around 95% of the edges have been rewired at least once. (c) The network after 400-time steps.

Here, the single parameter $p_1$ is called aversion bias [31], which denotes the tendency to cut connections between dissimilar agents. A higher $p_1$ value means that the agent maintains stronger connections to dissimilar agents.

## 4. Experiments

This section applies extensive experiments on various datasets to demonstrate the proposed method's dynamical performance and effectiveness. We use Python to do our experiments on a 2.9 GHz CPU and 16 G RAM computer. We first consider the segregation process on an ER random network [32], as specified in figure 3. Then, to explain the process of segregation in a real social network, our method is applied to the well-known Karate network as shown in figure 4. Furthermore, we develop network models for typical parameter values. Some indexes are used to quantify dynamical segregation, as shown in figure 5. We evaluate the quality and efficiency of network segregation using **LFC** and five different conventional methods on the BA network [33]. Figure 6 depicts our method's improved performance. We conducted 20 times for each experiment and averaged the experimental results to reduce errors.

Firstly, we apply the segregation process on an ER random network with 100 nodes and 300 edges and nodes partitioned into two groups with equal probability initially (i.e., the $\beta_i$ equals $k_i$ or $-k_i$ with 50% probability). The nodes with positive values of attributes are represented as purple, whereas others with negative values are represented as orange. The size of the node represents the degree. In the process of network evolution, when the edge length distribution reaches for the stationary distribution, the long edges with different attributes become short eventually. In the ultimate condition, as shown in figure 3(c), where the great majority of edges are short, which represents agents with tiny attribute distances.

Secondly, we apply segregation process to this famous Karate network, which is shown in figure 4. There are two key leaders, i.e., node 1 and node 34 are highlighted in figure 4. We do not fix key leaders in this segregation process and choose them by maximizing the leadership index. Interestingly, during the entire

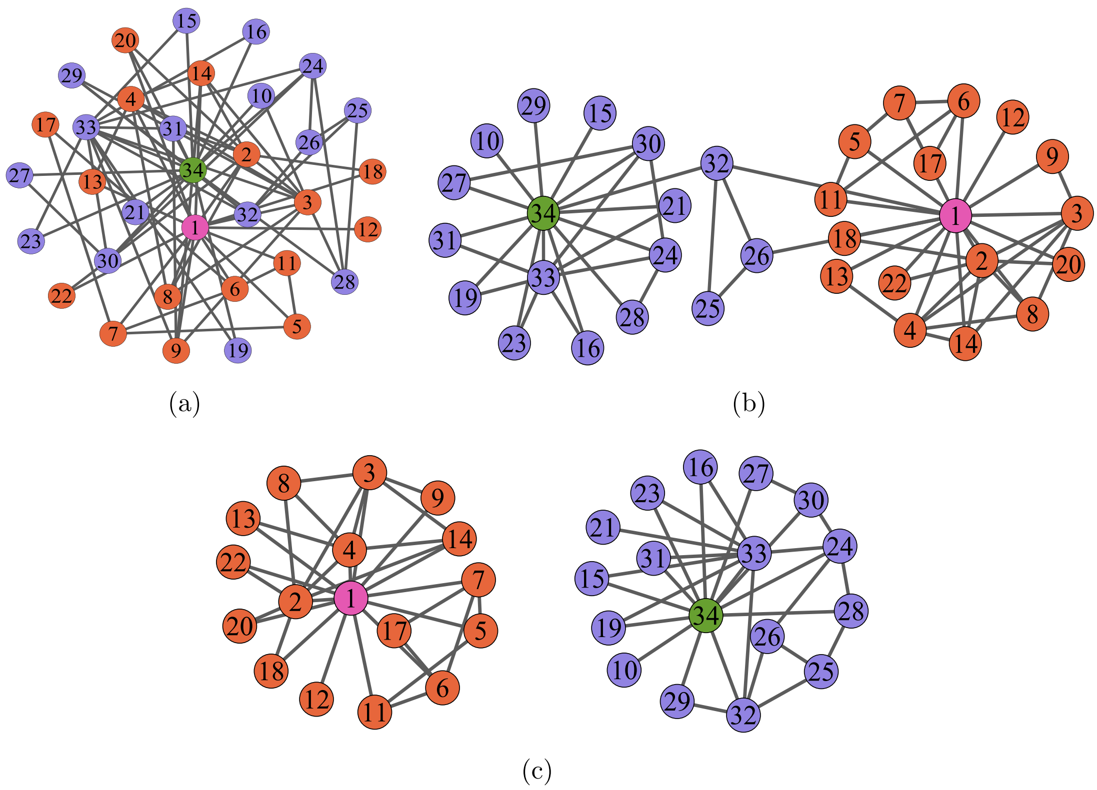


**Figure 4.** The segregation process driven by key leaders in Karate network. (a) The initial Karate network. (b) After 50 time steps, nearly 65% of the edges in the Karate network had been rewired at least once. (c) The Karate network after 150 time steps.

segregation process, nodes 1 and 34 are consistently recognized as leaders. It can be assumed that these leaders should not be conformists in the evolutionary process and their states are stable to a large extent. Our method can well explain the evolution process of Karate club gradually segregated into two groups under two leaders. Moreover, we can obtain that the state and attribute distribution of each node in the iterative procedure.

Then, to quantify this evolutionary process, we utilize a set of classical indexes to measure segregation [34] in complex networks. We exploit participation coefficient $P$ and modularity $Q$ to judge the extent of dynamical segregation. In addition, we apply global efficiency $E$ to evaluate the extent of dynamical integration. We apply these quality indexes to an ER random network (where $N = 1000$, $m = 3000$), with different $\delta$. The changes of these quantities show a monotonically increasing behaviour of $P$ (figure 5(a)), $Q$ (figure 5(b)), $E$ (figure 5(c)) and $r$ (figure 5(d)) with segregation. While a monotonically decreasing trend of $P$ (figure 5(a)) and $E$ (figure 5(c)) up to balanced when the whole network is completely segregated. As a result, the dynamical segregation or integration evaluated as the product of $P$, $Q$, $E$, and $r$ indicate the presence of topological heterogeneity. As demonstrated in figures 5(e) and (f), we find that there exists an obvious opposite trend of $P \times E$ and $Q \times E$.

We also conduct experiments on a BA network, and the trends are similar to the ER network. However, a shorter iteration time is required to achieve complete segregation on the BA network. This is because highly dependent relations will lead to the connections of new edges in the process of segregation dynamics. And the two nodes with weak dependent relations have fewer edges. Thus, a highly heterogeneous network is easier to control segregation.

Finally, in order to prove that it is more advantageous to segregate network by selecting key leaders through **LFC**, we compare to different centrality measures [35], i.e., DC, CC, page rank (PR), k-shell (KS), BC in a BA network (where $N = 1000$, $\langle k_m \rangle = 10$). We find that **LFC** can segregate the network with the higher modularity $Q$. Figure 6(a) shows the modularity $Q$ by different methods in a BA network (because the properties of the BA network are similar to the real network). DC and CC are second only to our method. This is because *leadership* can integrate multiple centrality indexes to contain rich topological information. Figure 6(b) shows the global efficiency $E$ of the integration network by different methods. The flow of information in the network becomes more difficult as the iterative number increases. **LFC** improves network segregation efficiency as compared to other methods.

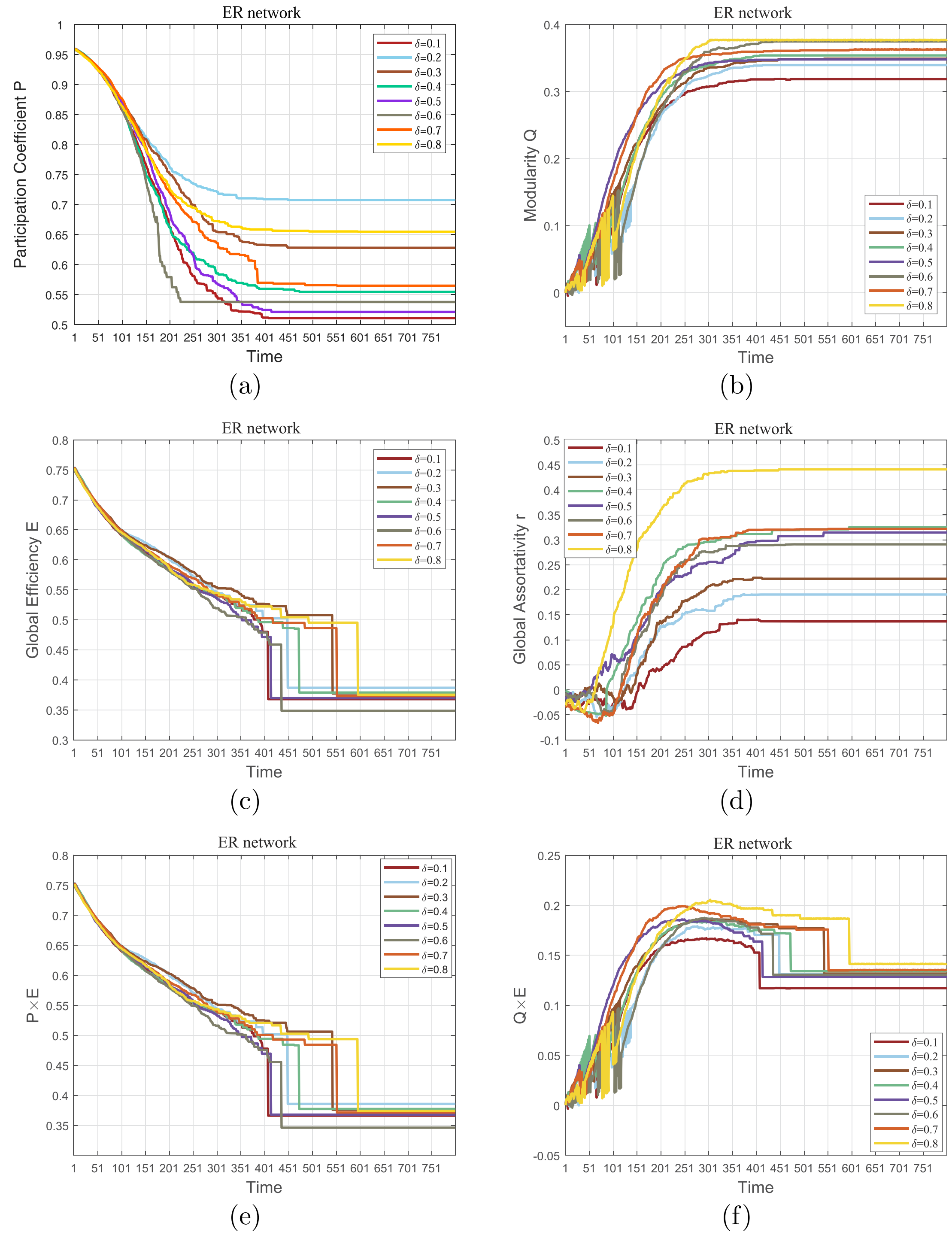


**Figure 5.** The changes of participation coefficient $P$ (a), modularity $Q$ (b), global efficiency $E$ (c), associativity coefficient $r$ (d), the production $P \times E$ (e) and $Q \times E$ (f) with different $\delta$ in ER network (where $N = 1000$, $m = 3000$).

Table 1 shows some statistical properties of BA networks ($N = 1000$). As is shown in tables 2 and 3, modularity $Q$ and global efficiency $E$ of network segregation as a function of the mean degree $\langle k_m \rangle$ in the BA networks ($N = 1000$) by distinct approaches. The lower value of $\langle k_m \rangle$ represents sparser linkages. Thus, for small $\langle k_m \rangle$ values, modularity $Q$ is small. All methods cannot segregate the network perfectly because it improperly identifies leader nodes and segregates with the sparse link. In other words, it generates extreme segregation. In addition, due to the increase of connection density between groups, the excessive segregation of groups decreases as $\langle k_m \rangle$ rises with the iteration of time. The larger value of $\langle k_m \rangle$, the more difficult it to find the key leaders and segregate the network correctly. With the increase of $\langle k_m \rangle$ and the network becomes denser, making it easier for information to flow in the network even in the process of network segregation. Thus, the global efficiency of network segregation decreases. Overall, our method can identify the key leaders more accurately and segregate the network more efficiently.

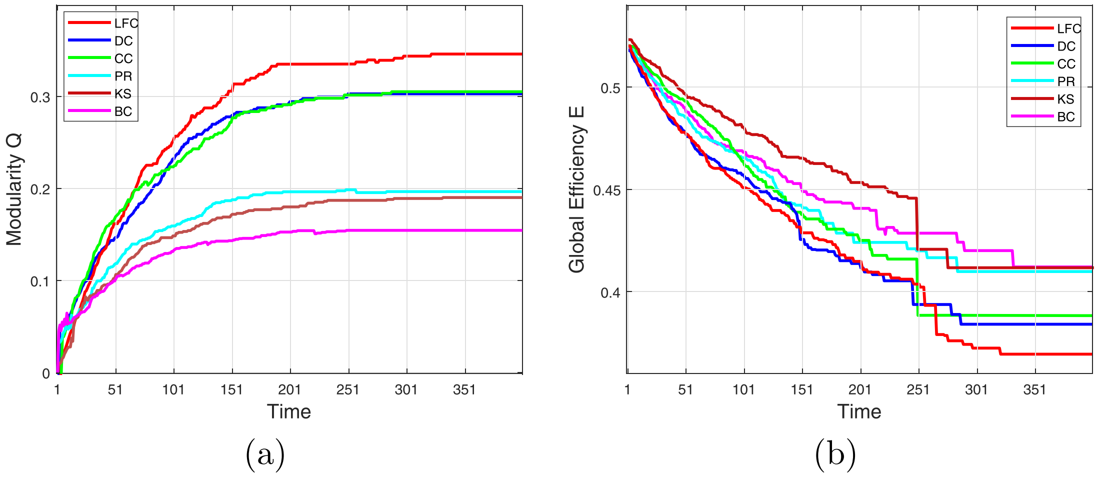


**Figure 6.** Modularity $Q$ and global efficiency $E$ of network segregation by different methods, as the iteration increasing, in the BA network ($N = 1000$, $\langle k_m \rangle = 10$). (a) Modularity $Q$. (b) Global efficiency $E$.

**Table 1.** Statistics properties of BA networks ($N = 1000$). $N$: the number of nodes; $\langle k_m \rangle$: the average degree; $M$: the number of edges; $c$: the average clustering coefficient; $\langle l \rangle$: the average short path length.

| $N$ | $\langle k_m \rangle$ | $M$ | $c$ | $\langle l \rangle$ |
|---|---|---|---|---|
| 1000 | 6 | 2991 | 0.032 | 3.483 |
| 1000 | 10 | 4975 | 0.041 | 2.972 |
| 1000 | 14 | 6951 | 0.049 | 2.743 |
| 1000 | 18 | 8919 | 0.056 | 2.611 |
| 1000 | 22 | 10 879 | 0.066 | 2.502 |

**Table 2.** Modularity $Q$ of network segregation by different methods, including: **LFC**, DC, CC, PR, KS, BC, as a function of the mean degree $\langle k_m \rangle$, in the BA network ($N = 1000$).

| $\langle k_m \rangle$ | **LFC** | DC | CC | PR | KS | BC |
|---|---|---|---|---|---|---|
| 6 | 0.5647 | 0.5639 | 0.5633 | **0.5658** | 0.5492 | 0.5545 |
| 10 | **0.5699** | 0.5641 | 0.5597 | 0.5543 | 0.5569 | 0.5438 |
| 14 | **0.5113** | 0.5093 | 0.5056 | 0.5082 | 0.5069 | 0.5046 |
| 18 | **0.4496** | 0.4389 | 0.4442 | 0.4482 | 0.4334 | 0.4273 |
| 22 | **0.2289** | 0.1939 | 0.2054 | 0.2143 | 0.1734 | 0.1685 |

**Table 3.** Global efficiency $E$ of network segregation by different methods, including: **LFC**, DC, CC, PR, KS, BC, as a function of the mean degree $\langle k_m \rangle$, in the BA network ($N = 1000$).

| $\langle k_m \rangle$ | **LFC** | DC | CC | PR | KS | BC |
|---|---|---|---|---|---|---|
| 6 | **0.1411** | 0.2135 | 0.2642 | 0.2735 | 0.2843 | 0.2735 |
| 10 | **0.4599** | 0.4711 | 0.4753 | 0.4788 | 0.4839 | 0.4941 |
| 14 | **0.5435** | 0.5534 | 0.5674 | 0.5872 | 0.5659 | 0.5712 |
| 18 | **0.5811** | 0.6107 | 0.6059 | 0.6173 | 0.6122 | 0.5013 |
| 22 | 0.6281 | **0.6139** | 0.6348 | 0.6173 | 0.6394 | 0.6395 |

## 5. Conclusions

This paper explored how key leaders promote the segregation process based on a multi-agent consensus system. It contributed to the transition from real networks to evolutionary models in these complex structures. The node's classification can simulate heterogeneous characteristics and aid to segregate networks. We proposed an index *leadership* to characterize the key leaders, and it could be extended to many notable centrality indexes, like DC, BC, CC, Katz centrality, KS, etc.

After identifying the key leaders, we evolved the network and decided whether to remove or rewire the edge depending on their attribute distance. The segregation dynamics on real and artificial networks showed that the dynamical model reveals the hidden dynamics of the collective system behaviours and predicts nodes' heterogeneous attributes. Furthermore, we will concentrate on empirical tests of models, focussing on assessing essential theoretical variables. Moreover, we will consider the network segregation of higher-order networks, such as signed networks and hyper-graphs.

## Acknowledgments

The National Natural Science Foundation of China (Grant No. 71871233) and Slovenian Research Agency (Grant Nos. P1-0403 and J1-2457).

## Data availability statement

All data that support the findings of this study are included within the article (and any supplementary files).

## ORCID iDs

Wenxuan Wang https://orcid.org/0000-0001-9986-1780
Yuhao Feng https://orcid.org/0000-0002-8047-6919
Wenzhe Xu https://orcid.org/0000-0002-0227-1678
Hui-Jia Li https://orcid.org/0000-0001-7969-548X
Matjaž Perc https://orcid.org/0000-0002-3087-541X

## References

[1] Girvan M and Newman M E J 2002 *Proc. Natl Acad. Sci. USA* **99** 7821–6
[2] DiPrete T A, Gelman A, McCormick T, Teitler J and Zheng T 2011 *Am. J. Sociol.* **116** 1234–83
[3] Tóth G *et al* 2021 *Nat. Commun.* **12** 1143
[4] Echenique F and Fryer R G 2007 *Q. J. Econ.* **122** 441–85
[5] Henry A D, Lubell M and McCoy M 2010 *J. Publ. Adm. Res. Theory* **21** 419–44
[6] Massey D S and Denton N A 1988 *Soc. Forces* **67** 281–315
[7] Kumpula J M, Onnela J-P, Saramäki J, Kaski K and Kertész J 2007 *Phys. Rev. Lett.* **99** 228701
[8] Han X, Cao S, Shen Z, Zhang B, Wang W-X, Cressman R and Stanley H E 2017 *Proc. Natl Acad. Sci. USA* **114** 2887–91
[9] Wang R, Liu M, Cheng X, Wu Y, Hildebrandt A and Zhou C 2021 *Proc. Natl Acad. Sci. USA* **118** e2104026118
[10] Tambuscio M, Oliveira D F M, Ciampaglia G L and Ruffo G 2018 *J. Comput. Soc. Sci.* **1** 261–75
[11] Siegel D A 2009 *Am. J. Pol. Sci.* **53** 122–38
[12] Schelling T C 1969 *Am. Econ. Rev.* **59** 488–93
[13] Schelling T C 1971 *J. Math. Sociol.* **1** 143–86
[14] Szolnoki A and Perc M 2016 *Sci. Rep.* **6** 23633
[15] Konig M D and Tessone C J 2011 *Phys. Rev.* E **84** 056108
[16] Zachary W W 1977 *J. Anthropol. Res.* **33** 452–73
[17] Li H-J, Wang L, Zhang Y and Perc M 2020 *New J. Phys.* **22** 063035
[18] Fortunato S 2010 *Phys. Rep.* **486** 75–174
[19] Boccaletti S, Ivanchenko M, Latora V and Pluchino A 2007 *Phys. Rev.* E **75** 045102
[20] Tan S Y, Wu J, Lü L, Li M J and Lu X 2016 *Sci. Rep.* **6** 1–9
[21] Zhou J and Chen Y-J 2015 *J. Econ. Theory* **157** 212–35
[22] Li H-J, Bu Z, Wang Z and Cao J 2020 *IEEE Trans. Ind. Inf.* **16** 5327–34
[23] Pastor-Satorras R and Vespignani A 2001 *Phys. Rev. Lett.* **86** 3200
[24] Xiao Y, Zhang N, Lou W and Hou Y T 2020 *IEEE Commun. Surv. Tutor.* **22** 1432–65
[25] Xie D, Yuan D, Lu J and Zhang Y 2013 *Trans. Inst. Meas. Control* **35** 426–36
[26] Bonacich P and Lloyd P 2001 *Soc. Netw.* **23** 191–201
[27] Carmi S, Havlin S, Kirkpatrick S, Shavitt Y and Shir E 2007 *Proc. Natl Acad. Sci. USA* **104** 11150–4
[28] Kitsak M, Gallos L K, Havlin S, Liljeros F, Muchnik L, Stanley H E and Makse H A 2010 *Nat. Phys.* **6** 888
[29] Rodriguez A and Laio A 2014 *Science* **344** 1492–6
[30] Henry A D, Prałat P and Zhang C-Q 2011 *Proc. Natl Acad. Sci. USA* **108** 8605–10
[31] Bosch-Domènech A and Silvestre J 2013 *Theory Decis.* **75** 465–96
[32] Boccaletti S, Latora V, Moreno Y, Chavez M and Hwang D U 2006 *Phys. Rep.* **424** 175–308
[33] Barabási A L and Albert R 1999 *Science* **286** 509–12
[34] Bojanowski M and Corten R 2014 *Soc. Netw.* **39** 14–32
[35] Lü L, Chen D, Ren X-L, Zhang Q-M, Zhang Y-C and Zhou T 2016 *Phys. Rep.* **650** 1–63